LA-9890-MS

Los Alamos National Laboratory is operated by the University of California for the United States Department of Energy under contract W-7405-ENG-36.

On Obtaining the Zero-Temperature Equation of State from Shock Data

Los Alamos

Los Alamos National Laboratory
Los Alamos, New Mexico 87545

LA-9890-MS

UC-34
Issued: January 1984

On Obtaining the Zero-Temperature Equation of State from Shock Data

B. I. Bennett

Los Alamos
Los Alamos National Laboratory
Los Alamos, New Mexico 87545

ON OBTAINING THE ZERO-TEMPERATURE EQUATION OF STATE FROM SHOCK DATA

by

B. I. Bennett

ABSTRACT

The Mie-Gruneisen theory of obtaining the zero-temperature equation of state from experimental shock wave data is reviewed. A study of certain commonly used forms of the Gruneisen parameter is made and the resulting equations of state are presented. These results indicate the limitations on the use of this procedure and suggest improvements for the calibration of pressure measurements in diamond anvil cells.

THE DIFFERENTIAL EQUATION

If experimental data of the pressure and density are available from shock wave experiments, it is possible, with some assumptions about the equation of state and the Gruneisen parameter Γ, to obtain the zero-temperature pressure (P_c) and energy (E_c) as a function of density. These thermodynamic quantities are sometimes referred to as the "cold curve."

To begin, we assume the equation of state is of the Mie-Gruneisen form. This usually requires that thermal excitation of internal degrees of freedom be small compared with the nuclear motion. With this assumption, the difference between the pressure on the Hugoniot (P_H) and P_c is related by $\Gamma(\rho)$ to the difference between the energy on the Hugoniot (E_H) and E_c.

$$P_H - P_c = \rho\Gamma(E_H - E_c) ,$$

where ρ is the density of the material in the shocked state. If we now assume that Γ is a known function, independent of E_c or its derivatives, and recall that P_c is related to the density derivative of E_c, the above is just a first-order differential equation for E_c.

$$\frac{dE_c}{d\rho} - \frac{\Gamma}{\rho}E_c = \frac{F(\rho)}{\rho^2} ,$$

where

$$F(\rho) = [(P_H - P_I) - \rho\Gamma(E_H - E_I)] + (P_I - \rho\Gamma E_I),$$

where P_I and E_I are the inital pressure and energy before to the shock. The restriction that $\Gamma(\rho)$ be independent of E_c or its derivatives precludes using this formalism in the Slater,[1,2] Dugdale-MacDonald,[3] or "free-volume"[4] expressions for $\Gamma(\rho)$. These particular expressions involve derivatives of the bulk modulus at zero temperature. The energy difference, $E_H - E_I$, is related by the Rankine-Hugoniot equations to the shock pressure using the following expression.[5]

$$E_H - E_I = \frac{1}{2}(P_H + P_I)\left(\frac{1}{\rho_I} - \frac{1}{\rho}\right) ,$$

where ρ_I is the initial density of the material. This produces an inhomogeneous term in the differential equation that is completely specified by experimental data and the known function $\Gamma(\rho)$.

$$F(\rho) = [P_H(\rho) - P_I]S_{1/2}(\rho) + P_I S_1(\rho) - \rho\Gamma(\rho)E_I ,$$

with $S_n(\rho) = 1 - n\Gamma(\rho)\left(\frac{\rho}{\rho_I} - 1\right)$.

The solution of this differential equation is straightforward to obtain, and the resulting expression for E_c may be used to give P_c, and the isothermal bulk modulus, (B_c).

$$E_c(\rho) = \Theta(\rho)\{ \int_{\rho_I}^{\rho} d\rho' \frac{F(\rho')}{\rho'^2\Theta(\rho')} + \frac{E_c(\rho_I)}{\Theta(\rho_I)} \} ,$$

$$P_c(\rho) = F(\rho) + \rho\Gamma(\rho)E_c(\rho), \text{ and}$$

$$B_c(\rho) = B_H(\rho)S_{1/2}(\rho) + \{(P_c(\rho) - P_I) - \frac{(P_H(\rho) - P_I))}{2}\} \Gamma(\rho) +$$

$$+ \{(E_c(\rho) - E_I) - (E_H(\rho) - E_I))\}\{\rho\frac{d}{d\rho}[\rho\Gamma(\rho)]\}.$$

The Debye temperature $\Theta(\rho)$ is defined here as $\Gamma(\rho) = d(\ell n \ \Theta)/d(\ell n \ \rho)$. The quantity $B_H(\rho)$ is the bulk modulus along the Hugoniot; $B_H(\rho) = \rho\{d[P_H(\rho)]/d\rho\}$.

The only variables that need specification are the thermodynamic quantities at the initial density. E_I may be chosen to be zero, thereby establishing the scale of the internal energy. P_I is 1 bar in most experiments conducted at ambient conditions. To specify the variable $E_c(\rho)$, we must make a further assumption about the equation of state.

For example, we might assume the material is a Debye solid. This is consistent with the original assumption that the material obeys a Mie-Gruneisen form for the equation of state. For this case, E_c at the initial density is given by the following expression:

$$E_c(\rho_I) = E_I - 3N_o k_B T\{D(\frac{\theta(\rho_I)}{T}) + \frac{3}{8}\frac{\theta(\rho_I)}{T}\} ,$$

where $D(x) = \frac{3}{x^3}\int_0^x dx' \frac{x'^3}{e^{x'} - 1}$, and $x = \theta/T$.

N_o is Avogadro's number, k_B is Boltzman's constant, and T is the temperature of the material before the shock.

With these assumptions, P_c, E_c, and B_c are expressed in terms experimental data. Since the bulk modulus along the Hugoniot (B_H) is not usually measured, this quantity must be obtained numerically from the pressures.

USING EXPERIMENTAL DATA

Experimentally, the quantities that are actually measured are the shock and particle speeds of the material (U_s and U_p). The Hugoniot pressure, energy, and density are related to these quantities by the following conditions:[5]

$$P_H - P_I = \rho_I U_s U_p \ ,$$

$$E_H - E_I = \frac{P_I}{\rho_I}\frac{U_p}{U_s} + \frac{1}{2}U_p^2 \ , \text{ and}$$

$$\rho = \rho_I\left(\frac{U_s}{U_s - U_p}\right) \ .$$

For most materials, the shock speed is nearly a linear function of the particle speed. Deviation from linearity is usually a consequence either of structural phase transitions with an appreciable volume change or of electronic excitations. Under these circumstances, the Mie-Gruneisen assumption is violated. An interesting discussion of these types of variation is found in Ref. 6. In what follows, we will assume the data for shock velocity versus particle velocity can be represented over some specified range by a quadratic form.

$$U_s = C_o + S\ U_p + R\ U_p^2.$$

The quantities C_o, S, and R are coefficients in the U_p expansion. The compression of the shocked material relative to the initial density is given as

$$\eta \equiv \frac{\rho}{\rho_I} = \frac{C_o + S\,U_p + R\,U_p^2}{C_o + (S-1)\,U_p + R\,U_p^2} \;.$$

In practice, we are interested in specifying a density and obtaining the cold-curve quantities. The above equation may be solved for U_p as a function, of compression, and then the quadratic form for U_s is evaluated. We then may evaluate the Hugoniot pressure and energy for use in the equations for the cold-curve quantities.

However, when $\eta = 1$, or if the coefficient R is nearly zero, the usual solution for U_p as a quadratic form is computationally unsuitable. Hence, it is convenient to express $U_p(\eta)$ by the following equations.

$$U_p(\eta) = \frac{U_{p\ell}(\eta)}{f(\eta)} \;,$$

$$U_{p\ell}(\eta) \equiv \frac{C_o(\eta - 1)}{\eta - S(\eta - 1)} \;, \text{ and}$$

$$f(\eta) \equiv \frac{1}{2}\{1 + [1 - W(\eta)]\} \;,$$

$$\text{where } W(\eta) = \frac{R}{C_o}[2U_{p\ell}(\eta)]^2 \;.$$

The quantity $U_{p\ell}(\eta)$ is the relationship connecting the particle velocity to the compression when the coefficient R is exactly zero. Under this condition, $f(\eta)$ is unity.

If such a quadratic expression is available from the data, then the bulk modulus can be convieniently expressed in terms of the fit parameters instead of requiring data for the pressure to be closely spaced so as to be differentiated numerically. Under this circumstance, B_H can be written as

$$B_H(\eta) = \rho_I C_o\{2U_s - C_o + R\, U_p^2\}\frac{1}{f(2f - 1)}\{\frac{\eta}{[\eta - S(\eta - 1)]^2}\} .$$

This equation implies that U_s, U_p, and f are evaluated at the compression η.

CHOOSING A GRUNEISEN PARAMETER

The procedure given above, along with a model for the motion of the atoms in the material, enables one to obtain the equation of state for the material from zero temperature up to and, in some circumstances, beyond the temperature reached in the shocked state. The obvious limitations are the model used for the atomic motion and whether the material truly obeys the Mie-Gruneisen form for an equation of state. The most important limitation is the choice of $\Gamma(\rho)$.

The Mie-Gruneisen formalism can produce unphysical results for the cold curve. This can be seen most directly in the expression for $F(\rho)$ and, in particular, that for $S_{1/2}(\rho)$. It is possible for $S_{1/2}(\rho)$ to become negative. When this occurs, $F(\rho)$ will be negative, thereby reducing the contribution to E_c by the integral, and explicitly giving a negative contribution to the pressure. The compression at which this happens depends upon the variation of $\Gamma(\rho)$.

To know exactly where such a divergence occurs requires a specified functional form for $\Gamma(\rho)$. The most commonly used forms all have this potential. As an example, we will consider the following expression for $\Gamma(\rho)$.

$$\Gamma(\rho) = \frac{\Gamma_I}{\eta^m} ,$$

where Γ_I is $\Gamma(\rho)$ at the initial density (i.e., $\eta = 1$), and m is an exponent of η assumed to be positive. This simple form is clearly not adequate for large compressions. However, it is used here for illustration since it encompasses a popular form used by some experimentalists, namely for m = 1 (or $\rho\Gamma$ = constant).

We now ask at what value of η for this choice of $\Gamma(\rho)$ will $S_{1/2}(\rho)$ vanish. Since we are only interested in shock compressed materials, only values of $\eta > 1$ need be considered. This query reduces to solving

$$\eta_o = 1 + \frac{2}{\Gamma_I}\eta_o^m \ .$$

We can separate the solutions into three classes: (1) $0 \leqslant m < 1$, (2) $m = 1$, (3) and $m > 1$. For class 1, solutions exist for the range of m implied:

$$1 + \frac{2}{\Gamma_I} \leqslant \eta_o \leqslant \infty.$$

For class 2, $S_{1/2}(\eta) = 0$ when $\eta_o = \Gamma_I/[\Gamma_I - 2]$, and finally, for class 3, no values for η make $S_{1/2}$ vanish.

The next item to consider is whether these special points lie within an experimentally reachable compression range. Values for Γ_I span a range of 1/2 to 3.[7,8] This gives values of η_o on the intervals $\{5/3,\infty\}$ for class 1; and $\{-1/3,3\}$ for class 2. Present experimental techniques can produce compressions of nearly threefold. Hence, in using such data and in selecting a $\Gamma(\rho)$, care must be taken to avoid forms that produce these artificial divergences.

Two other forms for $\Gamma(\rho)$ that have enjoyed popular use in hydrodynamic codes over the past 13 years are SESAME and CHART-D[9]:

$$\Gamma(\eta) = \frac{\Gamma_I}{\eta} + \frac{2}{3}\left[1 - \frac{1}{\eta}\right]^m ,$$

where $m = 1$ is the SESAME[a] form and $m = 2$ is the CHART-D form. Again, neither form is appropriate for very large compressions. These expressions also can cause behavior in the inferred cold curves similar to that in the previous discussion.

Finally, there is a model developed by R. G. Cowan at Los Alamos in 1957 derived from Thomas-Fermi-Dirac theory which has also been in use for several years.

$$\Gamma(\rho) = b + \frac{c}{1 + \xi(\rho)} ,$$

where $\xi(\rho) = a\rho/A$ (A is the atomic weight of the material). The constants a, b, and c are as follows:

$$a = 9\ Z^{0.3} ,$$

$$b = 0.6\ Z^{1/9} ,$$

$$c = 2 ,$$

and Z is the atomic number of the material.

Each of the above forms for $\Gamma(\rho)$ can be used, within the limitations mentioned about divergent solutions, to compute cold curves. To avoid the divergences, as the solutions are obtained for B_c, we stop when the derivative of B_c becomes negative. This precursor tells us when we are nearing the limiting compression.

[a] This form was devised by J. F. Barnes, Los Alamos Scientific Laboratory, c.a. 1970.

COMPARISON WITH BANDSTRUCTURE RESULTS

To assess the quality of the final result, an independent source for the cold curve is required. The most reliable theoretical method available is from electronic bandstructure calculations, which are quantum mechanical solutions that explicitly account for the crystal structure of the material.

The three materials chosen for comparison were aluminum, copper, and molybdenum. These materials have available extensive bandstructure calculations of the cold curve.[b,c,d] Moreover, a great number of shock measurements have been made on them over the years, and aluminum and molybdenum are used as impedence-matching standards for shock measurements on other materials.[10] Copper and molybdenum room-temperature isotherms are used as standards to calibrate the shift in ruby fluorescence as a function of pressure in static experiments using the diamond anvil cell.[11]

For each of these materials and for each $\Gamma(\rho)$ models discussed, the cold curves were obtained. Only linear fits to the shock data were used so R is zero. The following table summarizes the parameters used for the calculations.

---

[b] Provided by A. K. McMahan. These are APW calculations for fcc aluminum using the Hedin-Lundqvist exchange-correlation potential.

[c] Provided by R. C. Albers, A. K. McMahan, and J. E. Muller. These are APW calculations for fcc copper using the Hedin-Lundqvist exchange-correlation potential.

[d] Provided by R. C. Albers. These are LMTO calculations for bcc molybdenum using the von Barth-Hedin exchange-correlation potential.

	Al	Cu	Mo
ρ (g/cm^3)	2.698	8.934	10.220
C_o (km/s)	5.333	3.910	5.124
S	1.356	1.510	1.233
Γ_I	2.15	1.99	1.57
	1.477[e]	1.319[e]	1.416[e]
$\theta(\rho_I)$ (K)	420.0	344.5	440.0
	412.4[e]	683.2[e]	452.5[e]

---

[e] Γ_I and $\Theta(\rho_I)$ are provided by the Cowen model.

The results of these calculations are shown in Figs. 1 - 3. The range of densities shown approximates that discussed above to avoid divergences. The actual cutoff densities for the calculations are given in the table below. Graphical information beyond these densities are extrapolations based upon a simple approximation to Thomas-Fermi theory and should not be considered accurate.

Cutoff Densities for the Γ Models

ρ(g/cm^3)

	Al	Cu	Mo
CHART-D	5.3	18.1	21.8
SESAME	4.3	18.6	17.1
Cowan	4.7	19.3	15.4
$\rho\Gamma$ = const.	6.9	18.9	21.3

The points marked with crosses in Figs. 1-3 are the band theoretic results from McMahan, Albers, and Muller.

Three general observations can be extracted from these results:

1. All models for $\Gamma(\rho)$ give about the same results for pressures up to approximately half the value of the bulk modulus at the

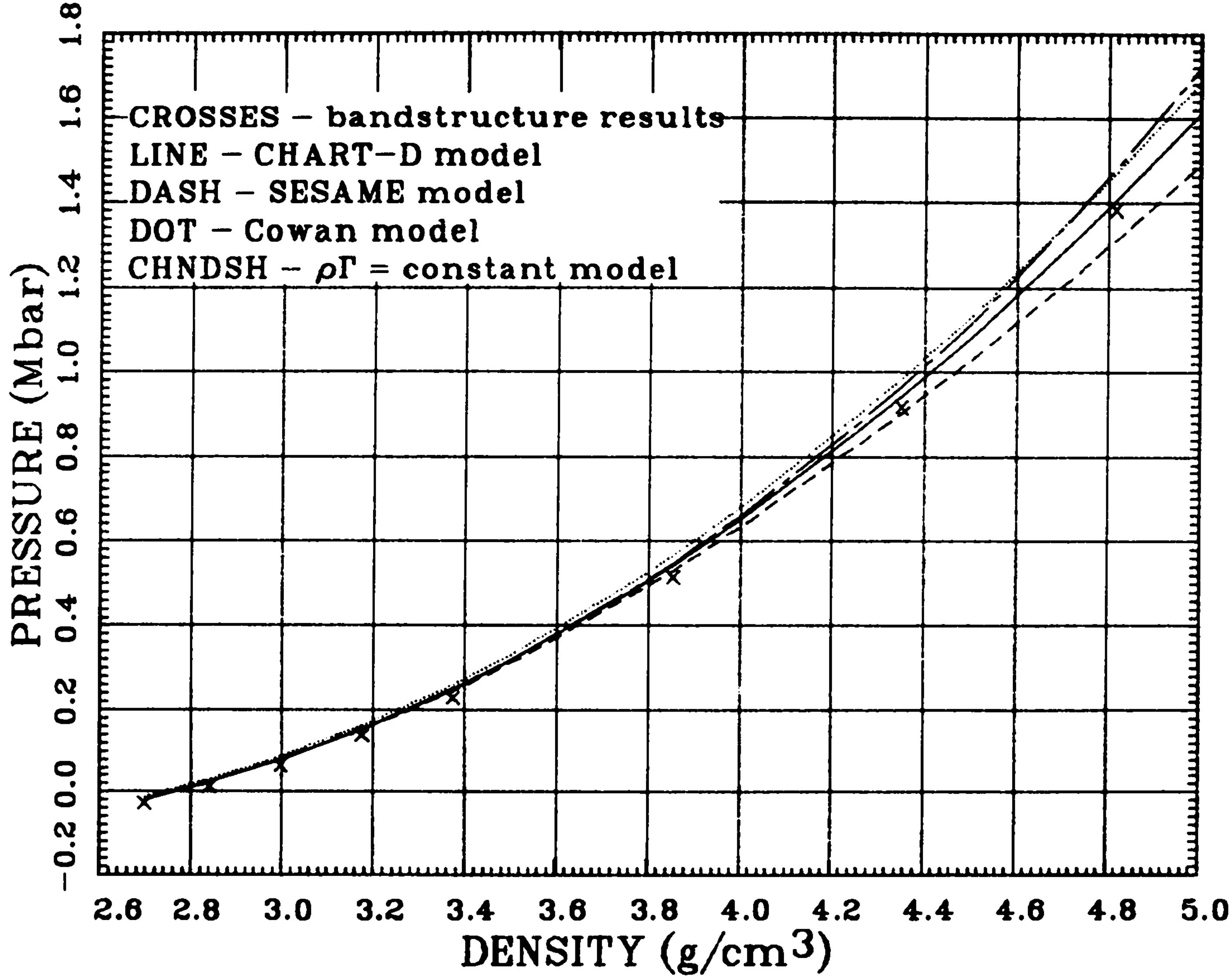

Fig. 1. Aluminum cold curves.

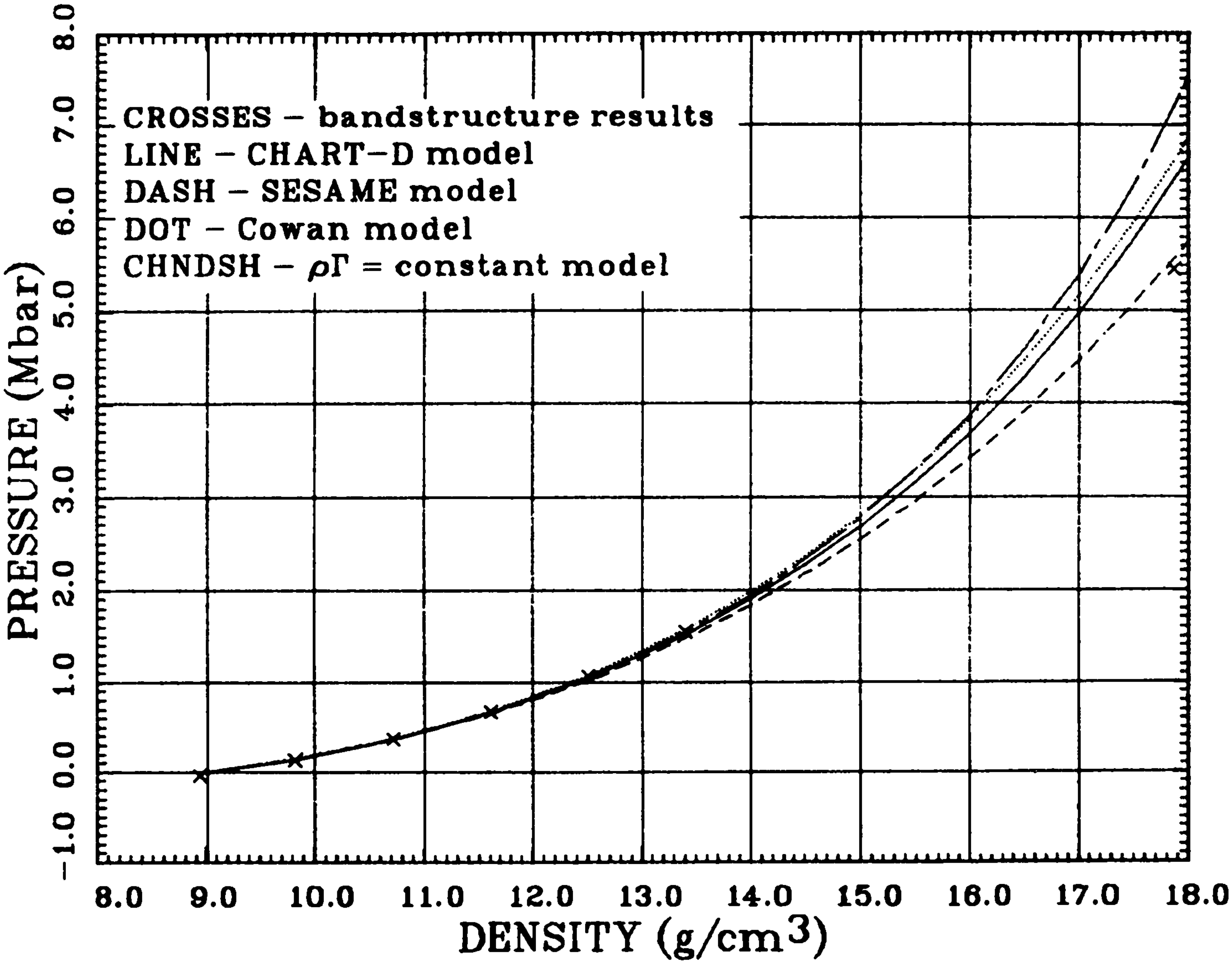

Fig. 2. Copper cold curves.

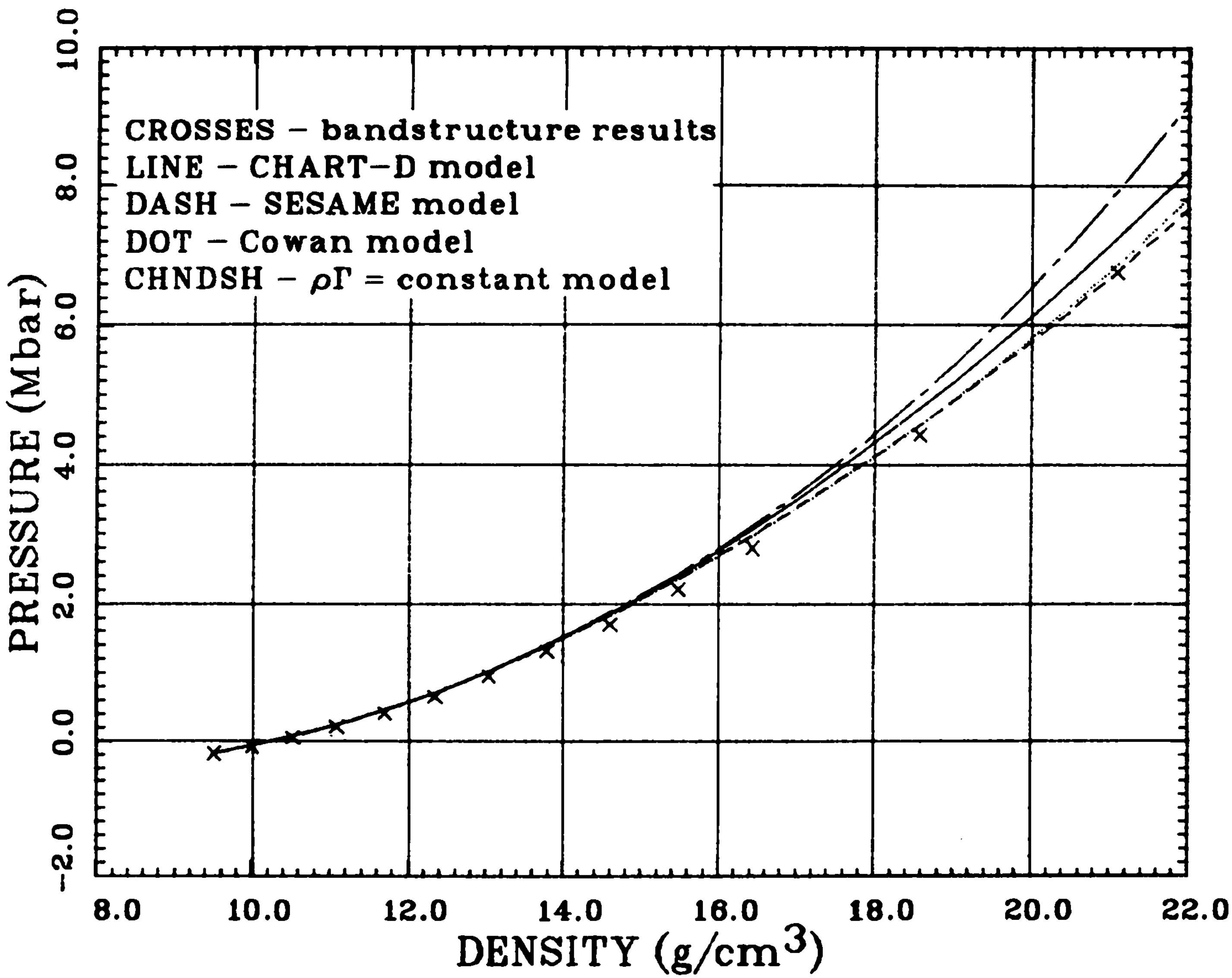

Fig. 3. Molybdenum cold curves.

initial density. For the materials considered this means aluminum, 350 kbar, copper, 650 kbar, and molybdenum, 1.3 Mbar.

2. For pressures below those mentioned, the procedures give fairly good agreement with the band theoretic results.

3. For pressures above those mentioned, the models are unpredictable and do not yield a reliable cold curve.

Near zero pressure, the band theoretic results have some uncertainty caused by the sensitivity to the choice of the exchange-correlation potential. However, at compressions higher than the zero pressure density this sensitivity becomes less important. The following observations ignore what happens at zero pressure.

For aluminum and molybdenum, there is a systematic trend of producing pressures that are about 10% too high. The copper results, when compared with the band theoretic pressures, are about 2% low.

The discrepancy in molybdenum affects the calibration of the ruby fluorescence pressure gauge. The room-temperature isotherm for molybdenum used in the calibration was derived from the Hugoniot data using the $\rho\Gamma$ = constant model.[10] There were slight differences in the choices of parameters for the calculation but the results of Ref. 10 and this work are essentially the same.

Examination of Fig. 3 of Ref. 11, shows a systematic trend for molybdenum to have pressures higher than those of the other calibration materials for the same shift in wavelength. If the room-temperature isotherm had been computed using the band theoretic cold curve, this deviation would have been corrected. Since the final calibration was based upon a least squares fit of wavelength shift vs pressure for copper, molybdenum, silver, and palladium, of which molybdenum represented about 25% of the data, it is not clear how much the fit would be changed. However, band theoretic calculations are needed for silver and palladium. With these cold curves, a complete set of room-temperature isotherms could be obtained and the fit recalculated. This will be the topic of a forthcoming article.

ACKNOWLEDGEMENT

I thank A. K. McMahan, R. C. Albers, and J. E. Muller for providing me their band theoretic calculations.

REFERENCES

1. J. C. Slater, Introduction to Chemical Physics (McGraw-Hill, New York, 1939).
2. L. D. Landau and K. P. Stanyukovich, DAN SSSR 46, 399 (1945).
3. J. S. Dugdale and D. K. C. MacDonald, Phys. Rev. 89, 832 (1953).
4. Hirschfelder, Curtiss, and Bird, Molecular Theory of Gases and Liquids (John Wiley and Sons, New York, 1954).
5. M. H. Rice, R. G. McQueen, and J. M. Walsh, "Compression of Solids by Strong Shock Waves," Solid State Physics 6, 1 (1958).
6. L. V. Al′tshuler, A. A. Bakanov, I. P. Dudoladov, E. A. Dynin, R. F. Trunin, and B. S. Chekin, "Shock Adiabatic Curves of Metals. New Data, Statistical Analysis, and General Laws," J. Appl. Mech. Tech. Phys. 22, 145 (1981).
7. K. A. Gschneider, Jr., Solid State Physics 16 275 (1964).
8. "Selected Hugoniots", Los Alamos Scientific Laboratory Report, LA-4167-MS (1969).
9. Samuel L. Thompson, "Improvements in the Chart-D Radiation-Hydrodynamic Code I: Analytic Equations of State," Sandia Laboratories report SC-RR-70-28 (1970).
10. W. J. Carter, S. P. Marsh, J. N. Fritz, and R. G. McQueen, "The Equation of State of Selected Materials for High-Pressure References," National Bureau of Standards Special Publication 326, 147 (1971).
11. H. K. Mao, P. M. Bell, J. W. Shaner, and D. J. Steinberg, J. Appl. Phys. 49, 3276 (1978).

Printed in the United States of America
Available from
National Technical Information Service
US Department of Commerce
5285 Port Royal Road
Springfield, VA 22161

Microfiche (A01)

Page Range	NTIS Price Code	Page Range	NTIS Price Code	Page Range	NTIS Price Code	Page Range	NTIS Price Code
001-025	A02	151-175	A08	301-325	A14	451-475	A20
026-050	A03	176-200	A09	326-350	A15	476-500	A21
051-075	A04	201-225	A10	351-375	A16	501-525	A22
076-100	A05	226-250	A11	376-400	A17	526-550	A23
101-125	A06	251-275	A12	401-425	A18	551-575	A24
126-150	A07	276-300	A13	426-450	A19	576-600	A25
						601-up*	A99

*Contact NTIS for a price quote.

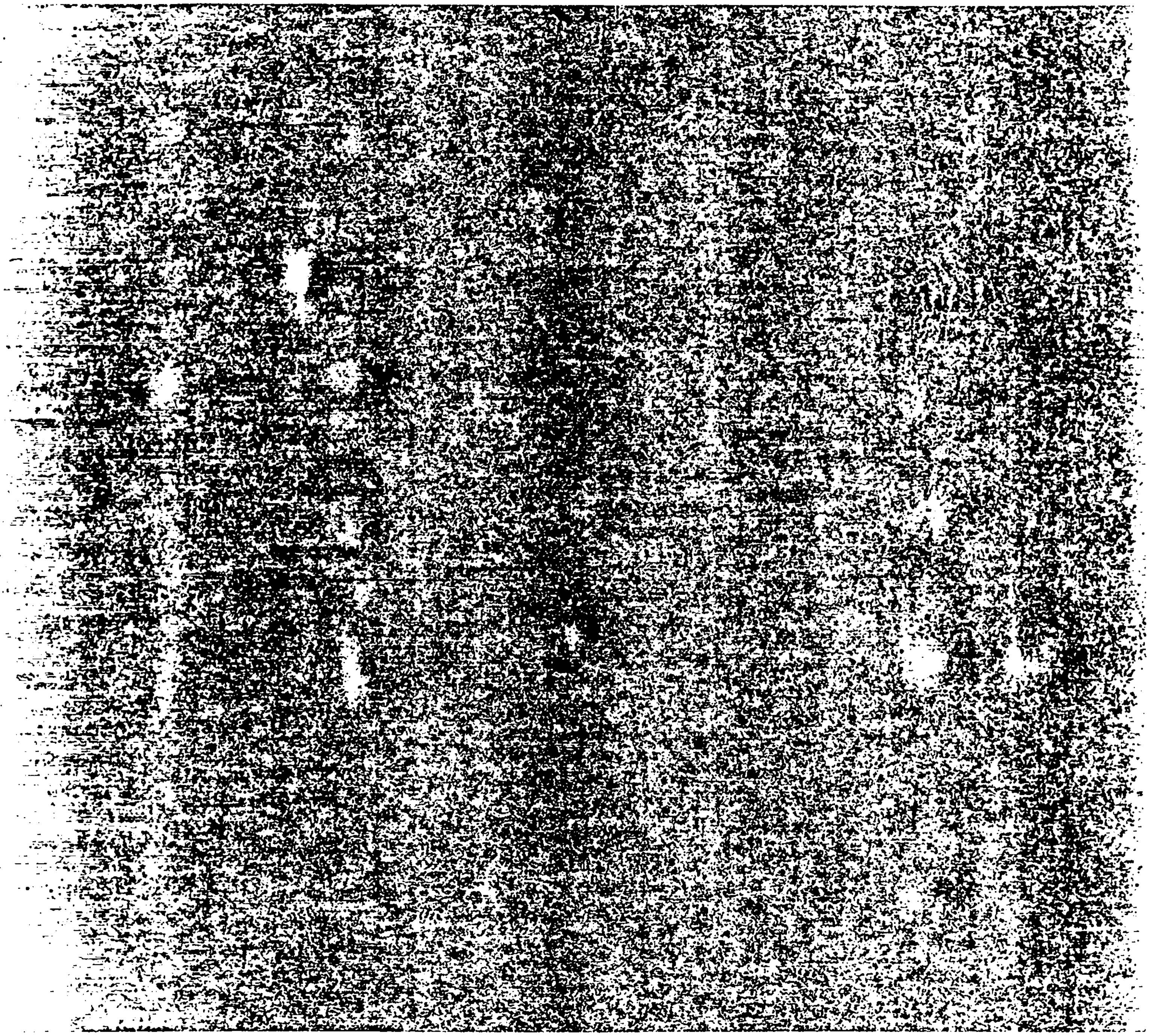

Los Alamos